Autoproteolytic activation of human aspartylglucosaminidase

Jani SAARELA*, Carita OINONEN†[1], Anu JALANKO*, Juha ROUVINEN† and Leena PELTONEN*[2]

*Department of Medical Genetics and National Public Health Institute, Department of Molecular Medicine, University of Helsinki, Haartmaninkatu 8, FIN-00290 Helsinki, Finland, and †Department of Chemistry, University of Joensuu, P.O. Box 111, FIN-87101 Joensuu, Finland

Aspartylglucosaminidase (AGA) belongs to the N-terminal nucleophile (Ntn) hydrolase superfamily characterized by an N-terminal nucleophile as the catalytic residue. Three-dimensional structures of the Ntn hydrolases reveal a common folding pattern and equivalent stereochemistry at the active site. The activation of the precursor polypeptide occurs autocatalytically, and for some amidohydrolases of prokaryotes, the precursor structure is known and activation mechanisms are suggested. In humans, the deficient AGA activity results in a lysosomal storage disease, aspartylglucosaminuria (AGU) resulting in progressive neurodegeneration. Most of the disease-causing mutations lead to defective molecular maturation of AGA, and, to understand the structure–function relationship better, in the present study, we have analysed the effects of targeted amino acid substitutions on the activation process of human AGA. We have evaluated the effect of the previously published mutations and, in addition, nine novel mutations were generated. We could identify one novel amino acid, Gly^{258}, with an important structural role on the autocatalytic activation of human AGA, and present the molecular mechanism for the autoproteolytic activation of the eukaryotic enzyme. Based on the results of the present study, and by comparing the available information on the activation of the Ntn-hydrolases, the autocatalytic processes of the prokaryotic and eukaryotic enzymes share common features. First, the critical nucleophile functions both as the catalytic and autocatalytic residue; secondly, the side chain of this nucleophile is oriented towards the scissile peptide bond; thirdly, conformational strain exists in the precursor at the cleavage site; finally, water molecules are utilized in the activation process.

Key words: activation mechanism, aspartylglucosaminidase, aspartylglucosaminuria, autocatalytic activation, Ntn-hydrolase, site-directed mutagenesis.

INTRODUCTION

Human aspartylglucosaminidase [AGA, N^4-(β-*N*-acetyl-D-glucosaminyl)-L-asparaginase, glycosylasparaginase; EC 3.5.1.26] is a lysosomal enzyme that belongs to the N-terminal nucleophile (Ntn)-hydrolase protein superfamily [1]. Other members of the Ntn-hydrolase superfamily with known structure are the proteasome β-subunit [2], glutamine 5-phosphoribosyl-1-pyrophosphate amidotransferase [3], penicillin G acylase [4], penicillin V acylase [5], cephalosporin acylase [6], and glutaryl 7-aminocephalosporanic acid acylase [7]. Most Ntn-hydrolase studies have been conducted with prokaryotic enzymes. Ntn-hydrolases are characterized by an N-terminal nucleophile that functions as the catalytic residue, which cleaves amide bonds in substrates. Despite the similarities in the catalytic process, the substrate specificities are very different for Ntn-hydrolases.

Enzymes belonging to the Ntn-hydrolase superfamily are synthesized as inactive polypeptides and undergo intramolecular autocatalytic activation. A range of autocatalytic events proceed via protein splicing [8], where the initial steps are thought to involve an N → O acyl rearrangement to generate a branched intermediate [9]. In Ntn-hydrolases, the hydrolysis of the peptide bond preceding the N-terminal active site residue by an autocatalytic rearrangement is similar to the initial step in the protein-splicing pathway. The same cleavage step generates the catalytically critical α-amino group. In Ntn-hydrolases, it is generally believed that the catalytic nucleophile also acts as the autocatalytic nucleophile [10–15]. Whether the nucleophile is threonine, serine or cysteine, Ntn-hydrolases share a common tertiary structure for the catalytic domain and equivalent stereochemistry at the active site [16,17]. The core three-dimensional folding pattern shared by Ntn-hydrolases consists of a four-layer $\alpha\beta\beta\alpha$-structure with two antiparallel β-sheets between α-helical layers.

The structure of the precursor is known for five Ntn-hydrolases: AGA, proteasome, penicillin G acylase, cephalosporin acylase and glutaryl 7-aminocephalosporanic acid acylase [12,14,18–21]. This information has been collected by analysing mutagenized native polypeptides with a prevented or delayed activation step. In addition, several other publications of Ntn-hydrolases have provided insights into the molecular details of precursor processing of AGA, glutaryl 7-aminocephalosporanic acid acylase, glutamine 5-phosphoribosyl-1-pyrophosphate amidotransferase, proteasome, and penicillin G acylase [10,11,13,15,22,23].

The three-dimensional structure of human AGA has been solved and the residues of the active site identified [1]. The critical catalytic residue is the nucleophile, Thr^{206}, which is stabilized by hydrogen bonds from Ser^{72} and Thr^{224}. The reaction intermediate is stabilized by hydrogen bonds from the side chain of Thr^{257} and main-chain nitrogen of Gly^{258}, while the substrate is bound by Arg^{234} and Asp^{237} [24], and possibly by Trp^{34} [25].

Dimerization and correct folding of the AGA precursor is a prerequisite for the activation of the precursor molecule. The residues critical for dimerization are located at the dimer interface [10,26,27]. The activation cleavage of the dimerized AGA precursors into the N-terminal α- and the C-terminal β-subunits takes place in the endoplasmic reticulum (ER) resulting in the tetrameric, enzymically active $(\alpha\beta)_2$ molecule. The activated AGA is transported to the lysosomes via the mannose 6-phosphate

Abbreviations used: AGA, aspartylglucosaminidase; AGU, aspartylglucosaminuria; ER, endoplasmic reticulum; Ntn, N-terminal nucleophile; rmsd, root mean square deviation; WT, wild-type.

[1] Present address: Department of Biochemistry, University of Kuopio, Savilahdentie 9, FIN-70211 Kuopio, Finland

[2] To whom correspondence should be addressed (e-mail Leena.Peltonen@ktl.fi).

pathway and the C-terminus of both subunits is trimmed by lysosomal hydrolases. This cascade of events in the biosynthesis of AGA has facilitated monitoring of the intracellular transport of the wild-type (WT) and mutated AGA molecules [28]. In general, the molecular and cellular biology of human AGA has been extensively studied since various mutations of AGA result in the lysosomal storage disorder aspartylglucosaminuria (AGU) [29].

The activation of AGA has been suggested to proceed via a *cis*-autoproteolysis of the precursor polypeptide and the event is influenced by the active site [24,30]. The integrity of the residues Asp^{205}–Thr^{206} at the subunit-processing site has been found to be crucial for efficient autoproteolysis of AGA [10,30]. Furthermore, some structural elements of the precursor of bacterial AGA indicate the existence of a strained *trans*-peptide bond between these residues [18]. Since strained peptide bonds at the activation site have also been observed for proteasome [20] and glutaryl 7-aminocephalosporanic acid acylase [19], a conformational strain at the activation site might contribute to the precursor activation.

The present study was designed to identify and verify experimentally the amino acids that are critical for the autocatalytic processing of human AGA. Amino acids in the immediate vicinity of the three-dimensional active site, as well as critical residues selected following structural comparisons with other members of the Ntn-hydrolase family, were selected for targeted mutagenesis and the folding, transport and catalytic kinetics of the synthesized AGA molecules were monitored.

MATERIALS AND METHODS

In vitro mutagenesis

Oligonucleotide-directed site-specific mutagenesis of the WT *AGA* cDNA in SVpoly expression vector [31] was performed using the QuikChange mutagenesis kit (Stratagene). The clones were sequenced with an ABI-Prism 377 DNA sequencer (PerkinElmer).

Transfection, metabolic labelling and immunoprecipitation

The methods used are as described by Saarela et al. [32]. In short, COS-1 cells [American Type Culture Collection (A.T.C.C.) strain CRL-1650] were transfected and, after 48 h, the cells were labelled for 1 h with [^{35}S]cysteine. A 1 h chase was followed by immunoprecipitation using AGA-specific polyclonal antibody against either the native enzyme (for most constructs) or the denatured subunits (for the $Gly^{226} \rightarrow$ Ala construct) [33]. The labelled polypeptides were separated by SDS/PAGE (14 % gels) under reducing conditions [34] and visualized by autoradiography.

Gel filtration

To resolve the tetrameric and dimeric AGA molecules, gel filtration of labelled polypeptides was performed as previously reported [10] on a Superdex 200 (10/30) column (Amersham Biosciences) after a 3 h chase. AGA polypeptides were immunoprecipitated from the collected fractions and analysed by SDS/PAGE and autoradiography.

Assay for AGA activity

The modified AGA activity assay [35] was performed after metabolic labelling. Cell lysate (10–30 μl) and 2 μl of 50 mM 2-acetamido-1-β-(L-aspartamido)-1,2-dideoxy-D-glucose (Sigma) were added to a final volume of 50 μl of 67 mM potassium phosphate buffer, pH 7.0, and incubated overnight at 37 °C. To stop the reaction, 107 μl of 5 % borate, pH 8.8, was added, and the sample was boiled for 5 min. Then, 1 ml of Ehrlich solution [0.1 g of 4-(dimethylamino)-benzaldehyde (Merck), 1 ml of hydrochloric acid and 10 ml of ethanoic acid] was added and the samples were incubated for 30 min at 37 °C. The amount of liberated *N*-acetylglucosamine was measured at 585 nm [36]. The K_m and V_{max} values were determined with substrate concentrations of 1, 2, 5, 10, 20, 30, 40 and 50 mM in three independent experiments for each concentration. The activities were correlated to the transfection efficiency as determined by co-expression of β-galactosidase using the β-galactosidase assay [37]. The protein amount was measured using the Bradford method [38], and clone-specific correlation was performed with quantification of immunoprecipitated radioactivity using an OptiPhase HiSafe3 liquid scintillation cocktail (PerkinElmer) with a Winspectral 1414 counter (Wallac, Evry, France). As a control for kinetic measurements, we used purified overexpressed WT human AGA enzyme.

Immunofluorescence analysis and confocal microscopy

The intracellular localization of AGA polypeptides was studied by staining the AGA transfected BHK-21 cells (A.T.C.C. strain CCL-10) with AGA-specific antibodies and fluorescent secondary antibodies (Jackson ImmunoResearch Laboratories) as described in [32]. Specimens were viewed with a 63× objective on a DMR confocal immunofluorescence microscope (Leica) with Leica NT software.

RESULTS AND DISCUSSION

Mutations of the AGA gene lead to a lysosomal storage disease, AGU. The cell-biological consequences of the disease mutations are often related to defective molecular maturation of AGA. To enhance our structure–function understanding of AGA, we have made an effort in the present study to evaluate if the previously published human AGA mutations could potentially affect the autocatalytic activation. In addition, nine novel mutations were generated based on their location in the active site. The effect of the mutations was monitored by immunoprecipitation- and immunofluorescence-based analysis of the expressed polypeptides, and the enzymic activity and kinetic parameters of AGA were measured. The results are summarized in Table 1. The data are presented and discussed using three categories of the amino acids: (i) the autocatalytic nucleophile, (ii) residues participating in autocatalysis, and (iii) residues with a structural role. The numbering of amino acids is according to the human AGA precursor and, where needed, corresponding bacterial amino acids are shown in parentheses. The previous results on human and bacterial AGA autocatalysis indicate that the mechanism is less efficient than in catalysis [10,30]. Thus the analysis of the autocatalytic mechanism using mutagenesis is more difficult and the results obtained are more indefinite.

The autocatalytic nucleophile Thr^{206}

The side chain of Thr^{206} functions as the catalytic group in AGA-catalysed substrate hydrolysis [1,25]. Its role in the autocatalysis has been defined thoroughly previously [10,18,25,39]. In autocatalysis, the hydroxyl oxygen of the Thr^{206} side chain forms a covalent bond to the carbonyl carbon of Asp^{205} probably resulting in a tetrahedral intermediate, which may be stabilized by an oxyanion hole (Scheme 1) [10,18]. The attack of the side chain of

Table 1 The processing, intracellular transport and activities of the WT and mutant AGA polypeptides in COS-1 cells

The intra- and extra-cellular AGA polypeptides seen on SDS/PAGE are listed in the immunoprecipitation column. The intracellular localization of AGA polypeptides are listed in the immunofluorescence column. The enzyme activity was determined from measurements using 2–5 mM substrate. The kinetic values K_M and V_{max} were determined using a range of different substrate concentrations and the standard deviation figures are each based on three measurements. The novel mutations are indicated in boldface type. Prec., precursor polypeptide; P, present; ND, not determined; BG, background.

	Immunoprecipitation						Immunofluorescence					
Construct	Prec.	Pro-α	α	Pro-β	β	β'	ER	Golgi	Lysosomes	Activity (% of WT)	K_m ($\pm$S.D.) (μM)	V_{max} ($\pm$S.D.) (μmol/min per mg)
WT AGA	P	P	P		P	P		P	P	100	444 $\pm$ 63	1.89 $\pm$ 0.33
Thr^{33} → Ala	**P**	**P**	**P**		**P**	**P**		**P**	**P**	**48**	**752 $\pm$ 139**	**1.63 $\pm$ 0.31**
Thr^{33} → Ser*	P	P	P		P	P	ND	ND	ND	100	ND	ND
Trp^{34} → Phe*/Ser	P	P	P		P	P	ND	ND	ND	14	ND	ND
Asp^{70} → Ala	**P**	**P**	**P**		**P**	**P**	**P**	**P**	**P**	**44**	**343 $\pm$ 79**	**1.23 $\pm$ 0.29**
Ser^{72} → Pro†	P		P	P			P	P	P	BG	ND	ND
Ser^{72} → Ala‡		P	P		P	P	ND	ND	ND	52‡	100 % WT‡	40 % WT‡
Asp^{200} → Ala	**P**	**P**	**P**		**P**	**P**		**P**	**P**	**87**	**480 $\pm$ 137**	**1.80 $\pm$ 0.27**
Asp^{201} → Ala	**P**	**P**	**P**		**P**	**P**		**P**	**P**	**93**	**464 $\pm$ 114**	**1.83 $\pm$ 0.35**
His^{204} → Gly§/Ser†	P	P	P	P			ND	ND	ND	30	ND	ND
Asp^{205} → Ala§/Gly/Ser	P		P	P			ND	ND	ND	BG	ND	ND
Thr^{206} → Ala§/Cys	P	P	P				ND	ND	ND	BG	ND	ND
Thr^{206} → Ser*	P	P	P		P	P	ND	ND	ND	BG	ND	ND
Thr^{224} → Ala‡	P	P	P		P	P	ND	ND	ND	BG	ND	ND
Thr^{224} → Ser‡		P	P		P	P	ND	ND	ND	21‡	100 % WT‡	28 % WT‡
Asn^{225} → Ala	**P**	**P**	**P**		**P**	**P**	**P**	**P**	**P**	**45**	**915 $\pm$ 178**	**1.86 $\pm$ .0.42**
Gly^{226} → Ala							**P**			**BG**	**4930 $\pm$ 2508**	**0.18 $\pm$ 0.12**
Gly^{226} → Asp‖	P		P	P			P	P	P	BG	ND	ND
Lys^{230} → Ala	**P**	**P**	**P**		**P**	**P**	**P**	**P**	**P**	**86**	**607 $\pm$ 101**	**1.87 $\pm$ 0.33**
Arg^{234} → Ala‡/Lys/Gln†	P		P	P			ND	ND	ND	BG	ND	ND
Asp^{237} → Ala‡/Ser	P	P	P		P	P	ND	ND	ND	BG	ND	ND
Ser^{238} → Ala	**P**	**P**	**P**		**P**	**P**	**P**	**P**	**P**	**40**	**1340 $\pm$ 272**	**1.18 $\pm$ 0.23**
Thr^{257} → Ala‡	P		P	P			ND	ND	ND	BG	ND	ND
Thr^{257} → Ile‖	P		P	P			P	P	P	BG	ND	ND
Thr^{257} → Ser‡		P	P		P	P	ND	ND	ND	70‡	100 % WT‡	63 % WT‡
Gly^{258} → Ala	**P**		**P**	**P**			**P**	**P**	**P**	**BG**	**4771 $\pm$ 2127**	**0.16 $\pm$ 0.07**
COS-1										BG (< 7)	4942 $\pm$ 2473	0.09 $\pm$ 0.06
Purified WT		P	P		P	P	ND	ND	ND	100	143 $\pm$ 21	2.17 $\pm$ 0.23

* [25].
† [35].
‡ [24].
§ [10].
‖ [32].

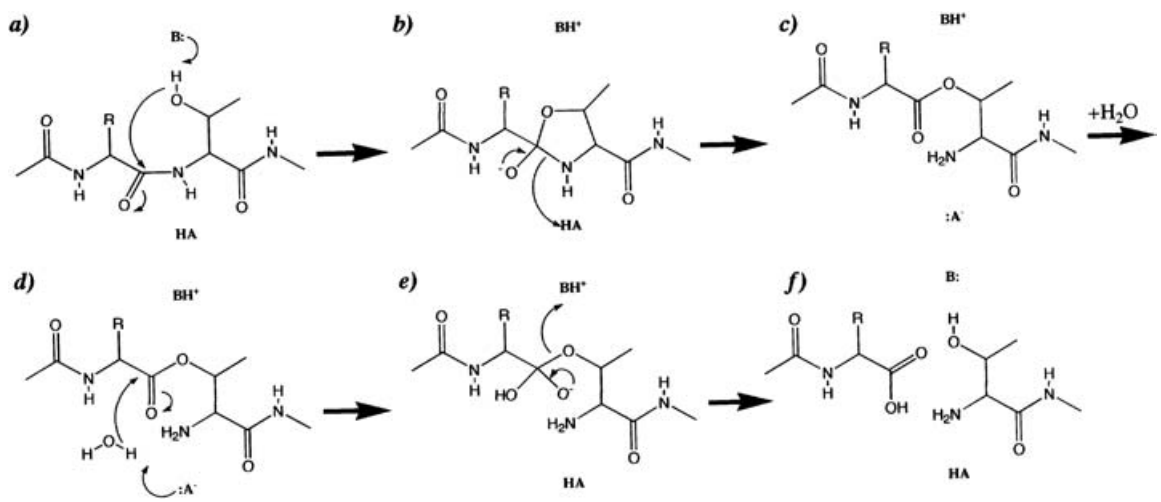

Scheme 1 Activation mechanism of human AGA

The activation is initiated by a general base (**a**), which receives the hydrogen atom from the side chain of Thr^{206}, thus enabling a nucleophilic attack on the carbonyl carbon of Asp^{205} and resulting in a tetrahedral intermediate (**b**). (**c**) An N → O acyl shift occurs and a general acid donates a proton to a newly formed amino group of Thr^{206}. (**d**) A water molecule hydrolyses the resulting ester bond and a second tetrahedral intermediate is formed (**e**). (**f**) The intermediate is resolved and Thr^{206} with free amino and side-chain groups is ready for enzymic catalysis. The identity of the general acid and base are discussed in the text.

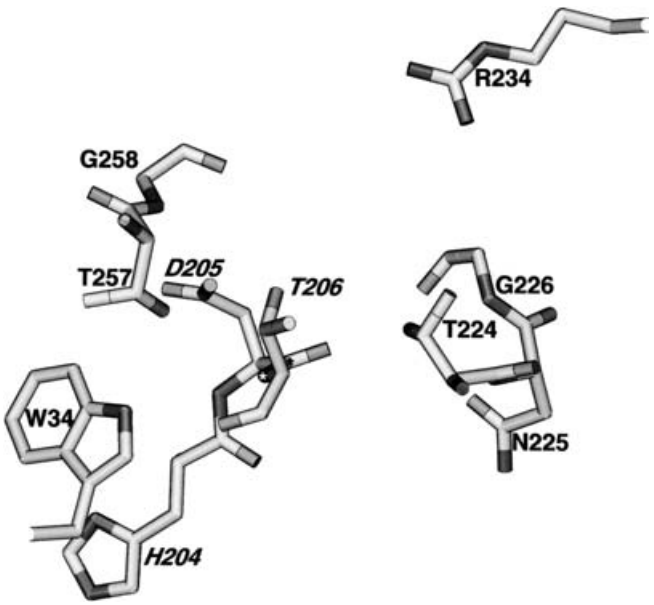

Figure 1 The most important active-site residues for the activation from human WT AGA structure

The propeptide residues His^{204} (His^{150}) and Asp^{205} (Asp^{151}) and the nucleophile Thr^{206} (Thr^{152}) have been taken from the inactive bacterial precursor AGA structure (PDB code 9gaf) and are written in italics. The strained peptide bond between Asp^{205} and Thr^{206} is scissile.

Thr^{206} is assisted by a general base. Some of the bacterial AGA precursor structures contain a high-energy distorted *trans* peptide bond between Asp^{205} and Thr^{206} (Asp^{151} and Thr^{152}) (Figure 1) [18], which is a potential driving force in the N → O shift [10,18,26]. Accordingly, conformational strain of the activation site is reported in proteasome [20] and glutaryl 7-aminocephalosporanic acid acylase [19]. Oligomerization of AGA precursor molecules is a prerequisite for activation [10,26,27]. Oligomerization may create conformational strain in the activation site, which is released by the cleavage of the scissile peptide bond.

Residues participating in autocatalysis

An acid and a base are required for the autoproteolytic activation of the AGA precursor into α- and β-subunits and the exposure of Thr^{206} (Scheme 1). Most studies of Ntn-hydrolase precursors report a water molecule as the general base [12,19,20]. In the case of bacterial precursor AGA, Asp^{205} (Asp^{151}) was proposed to act as the general base that was hydrogen-bonded to the nucleophile in one precursor structure [Protein Data Bank (PDB; http://www.rcsb.org/pdb/) code 9gaf] [18]. As discussed below, the position and conformation of Asp^{205} varies with different bacterial AGA precursor mutants. Thus it is possible that, for human AGA as well, the general base may be a water molecule [10]. The only role of Asp^{205} in activation may be to provide strain at the scissile Asp^{205}–Thr^{206} peptide bond. In the WT human AGA structure [1], the best candidate water molecule is hydrogen-bonded to Thr^{206} and Asp^{237}. It has been proposed that this neighbouring water molecule hydrolyses the ester bond resulting from the N → O shift and finally resolves the α- and β-subunits of AGA [10,18].

The tetrahedral transition state of AGA (Scheme 1b and 1e) may be stabilized by one or two hydrogen bonds, the so-called oxyanion hole. In Ntn-hydrolases, several oxyanion-hole-forming residues that use side-chain hydroxyl groups or nitrogen atoms of the main chain have been proposed [12–15,18–20]. For activation, an oxyanion hole is required in both the acylation and deacylation steps. In bacterial precursor AGA, Thr^{224} (Thr^{170}) may stabilize the reaction transition state by forming the oxyanion hole during activation (Scheme 1b and 1e) [18]. Previous studies of human AGA suggest that a hydroxyl group at Thr^{224} is important for autoproteolysis [24] and thus Thr^{224} may stabilize the reaction transition state by forming the oxyanion hole. However, as the precursor structures of bacterial AGA differ at the scissile Asp^{205}–Thr^{206} peptide bond, it is unclear whether Thr^{224} truly stabilizes the reaction intermediate or if it has a structural role.

Residues with a structural role

Structural comparison of Ntn-hydrolases has revealed eight fully conserved secondary-structure elements [17], all located in the β-subunit of the active AGA molecule. Two conserved or similar residues were identified within these secondary-structure elements: Gly^{258} and Gly^{226}. In addition to the AGAs of various species (human AGA; PDB code 1apy), Gly^{258} is conserved also in some other Ntn-hydrolases [proteasome from *Saccharomyces cerevisiae* (PDB code 1ryp, chain pre2), and *Escherichia coli* glutamine amidotransferase (PDB code 1ecf)], whereas penicillin acylase from *E. coli* (PDB code 1pnk) has alanine at this position in the conserved β-strand. At the position corresponding to Gly^{226}, only hydrophobic residues are found in other Ntn-hydrolases [17], whereas Gly^{226} is fully conserved in the AGAs of several species [32]. Gly^{258} and Gly^{226} are shown underlined in Figure 2. The backbone torsion angles of both Gly^{258} and Gly^{226} are abnormal in the human WT structure (Gly^{258}: $\Phi = 139$, $\psi = -141$; Gly^{226}: $\Phi = 84$, $\psi = -157$).

The main-chain nitrogen of Gly^{258} and the side chain of Thr^{257} form the human AGA oxyanion hole that is utilized in the stabilization of the negatively charged carbonyl oxygen on the transition state during enzyme catalysis [1]. We produced the Gly^{258} → Ala substitution and observed the marked precursor accumulation after metabolic labelling, immunoprecipitation, and SDS/PAGE (Figures 3 and 4), as well as strong immunofluorescence staining of the ER of the transfected COS-1 cells (data summarized in Table 1). However, some lysosomes were immunostained, implying a delayed transport of the mutated polypeptides to the lysosomes. The precursor polypeptide was examined further by gel filtration and subsequent immunoprecipitation. The results indicate the existence of both dimeric and monomeric precursor molecules (Figure 5). The amount of precursor polypeptide in the Gly^{258} → Ala cell and medium fractions compared with the WT was quantified further after gel filtration. The fractions containing the dimeric AGA molecule (> 57 kDa), contained 5-fold amounts of precursor in the mutant when compared with the WT. Similarly, the fractions representing the monomeric AGA molecules (< 44 kDa) contained 12-fold amounts of precursor in the mutant. The enzyme activity was comparable with the COS-1 cell background. The mutant polypeptides are probably unable to fold correctly and get mostly retained in the ER. The results indicate that Gly^{258} has a crucial structural role for the proteolytic cleavage and the activation of the human AGA precursor. The existence of a hydrogen bond between the main chain of Gly^{258} (Gly^{204}) and Asp^{205} (Asp^{151}) in three bacterial precursor structures (PDB codes 9gaa, 9gac and 9gaf) would indicate that a potential role of Gly^{258} might be stabilization of the intermediate in autocatalysis. However, the Asp^{205} mutants of the bacterial precursor have a very different conformation at Asp^{205}, and thus it would be speculative to conclude that, during human precursor activation, the main-chain nitrogen of Gly^{258} might stabilize the intermediate.

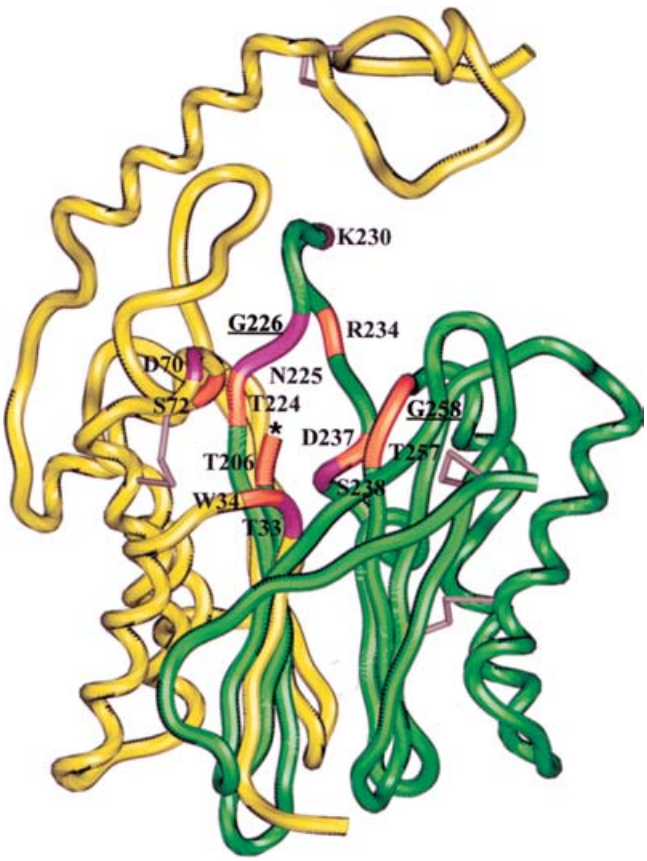

Figure 2 The backbone structure of a WT human AGA $\alpha\beta$-dimer

Only one heterodimer from the active $(\alpha\beta)2$ tetramer is shown. The α-subunit is coloured yellow and the β-subunit is coloured green. An asterisk marks the catalytically and autocatalytically active N-terminal Thr^{206}, which is revealed by the autocatalytic cleavage. Disulphide bridges are shown in light pink. The residues involved in enzymic catalysis or substrate binding are shown in orange. Mutagenized residues based on vicinity to the active site or conservation in Ntn-hydrolases are shown in purple or underlined respectively. The residues in the linker peptide between the α- and β-subunits, including the mutagenized residues Asp^{200} and Asp^{201}, are not shown.

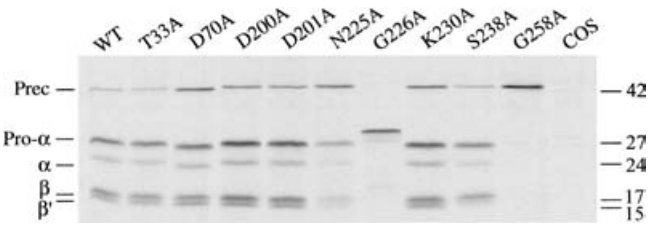

Figure 3 SDS/PAGE analysis of the processing of the WT AGA and mutated polypeptides

COS-1 cells transfected with different AGA cDNA constructs were labelled with [^{35}S]cysteine for 1 h and chased 1 h. The labelled cells were lysed, and the polypeptides were immunoprecipitated. The samples were analysed by SDS/PAGE (14 %) under reducing conditions. Mutants are indicated using one-letter amino acid codes, e.g. T33A is $Thr^{33} \rightarrow Ala$. Prec, precursor polypeptide.

The AGU-disease-causing $Gly^{226} \rightarrow Asp$ mutation results in abnormal processing of the AGA precursor and produces an inactive molecule, which is, however, correctly folded and transported to the lysosomes [32]. Gly^{226} resides in a loop in the active site and the substituting aspartate disturbs local folding by eliminating a tight turn of the loop and presenting a larger

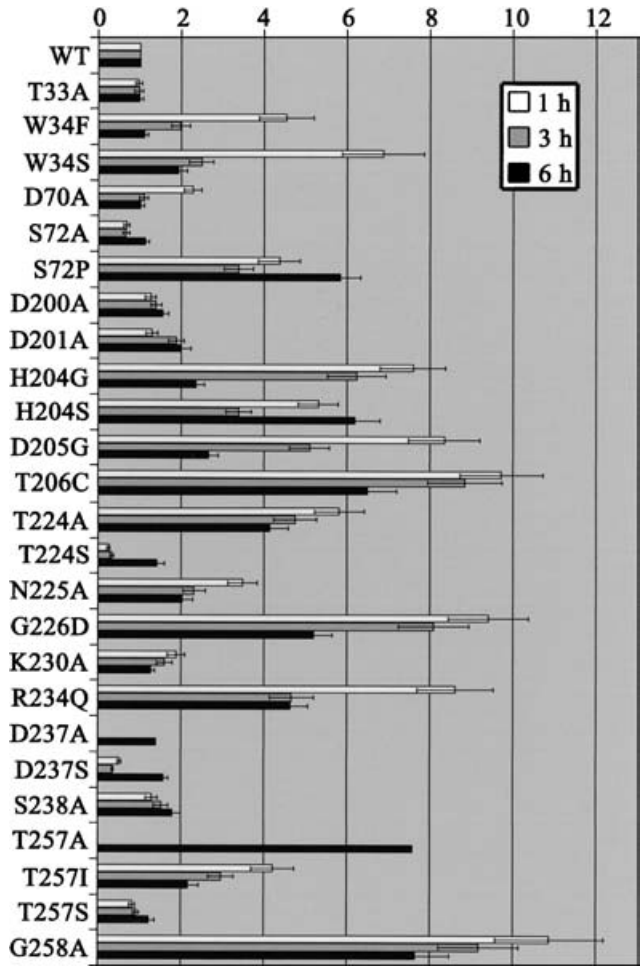

Figure 4 The amount of precursor polypeptide compared with the WT after 1, 3 and 6 h chase

The AGA polypeptides of scanned autoradiographs were quantified using the Scion Image software (Scion Corporation). The relative amount of the precursor polypeptide of the whole AGA polypeptide pattern of each mutant was compared with the WT analysed from the same autoradiograph. Each polypeptide species (except $Asp^{237} \rightarrow Ala$ and $Thr^{257} \rightarrow Ala$) was analysed three times and the error bars are shown. Mutants are indicated using one-letter amino acid codes, e.g. T33A is $Thr^{33} \rightarrow Ala$.

side chain in the aqueous environment of the substrate-binding funnel. We observed in the present study that the $Gly^{226} \rightarrow Ala$ mutation shows a more severe defect, since no normal subunit structure could be observed on SDS/PAGE (Figure 3). In immunofluorescence analysis, only the ER was stained with antibodies against the denatured subunits of AGA, which is evidence for the accumulation of the polypeptides in the ER (Table 1). The main-chain nitrogen of Gly^{226} (Gly^{172}) is hydrogen-bonded with the side chain of Thr^{224} (Thr^{170}) in the human and bacterial AGA structures. The side chain of Asp^{226} or Ala^{226} would point towards the residues Thr^{224}, Lys^{230} and Asp^{88} and create clashes. It is possible that the aspartate side chain could stabilize the structure by creating electrostatic interactions with Lys^{230}. A lack of such stabilization would create a major folding defect like that observed in the $Gly^{226} \rightarrow Ala$ mutant. The abnormal-size major band and the faint bands would suggest that the proteolytic activity in COS-1 cells has cleaved the precursor.

$Ser^{238} \rightarrow Ala$ and other novel mutations generated here, as justified by their position close to the active site, are shown in purple in Figure 2. The $Ser^{238} \rightarrow Ala$ substitution resulted in

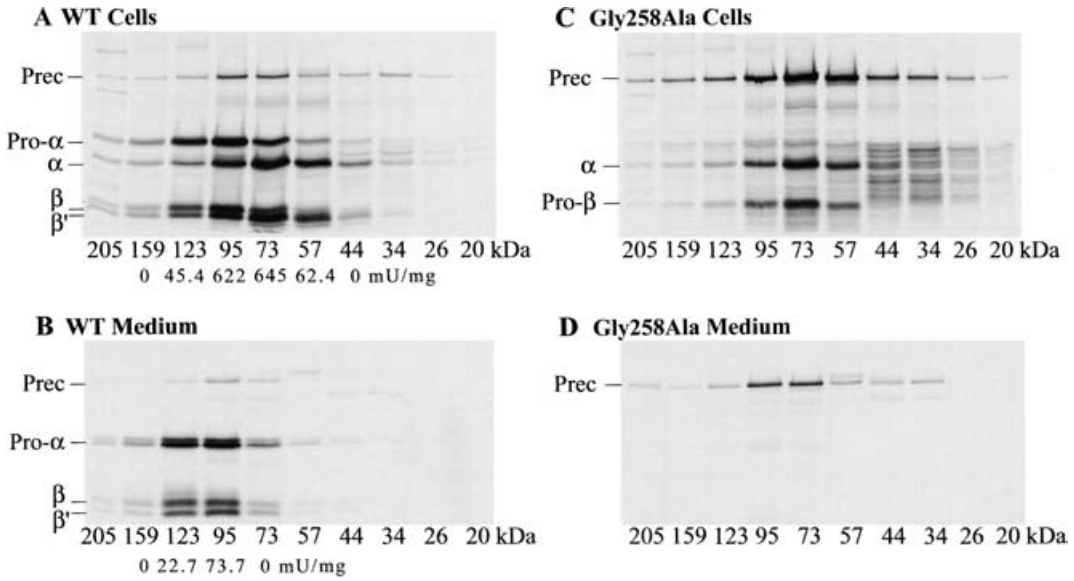

Figure 5 SDS/PAGE analysis of the gel-filtrated AGA polypeptides

Labelled polypeptides were collected from the cells and concentrated from the medium. Gel filtration was performed with a Superdex 200 column. Fractions corresponding to polypeptides with molecular masses between 200 and 20 kDa were immunoprecipitated. Samples were analysed by SDS/PAGE (14 % gels) under reducing conditions. (**A**) WT cells, (**B**) WT medium, (**C**) $Gly^{258} \rightarrow$ Ala cells and (**D**) $Gly^{258} \rightarrow$ Ala medium. The activities of the WT fractions are shown (in m-units/mg). Prec, precursor polypeptide.

delayed processing of the precursor (Figures 3 and 4). The activity measurements showed an increased K_m value and a decreased V_{max} value. Using immunofluorescence, the precursor polypeptides were seen both in the ER and lysosomes (Table 1). Due to the substrate-binding role of the neighbouring Asp^{237}, this particular substitution most probably has local structural consequences that affect enzymic catalysis. The general delay in folding thus resembles that observed for $Asp^{237} \rightarrow$ Ala.

Other novel mutations close to the active site seem to have a minor effect on activation. Replacement of Asp^{70} and Lys^{230} with alanine resulted in a small delay on precursor cleavage, yet after a 6 h chase, the precursor amount was at the level of that of the WT (Figures 3 and 4). A slight difference in size was systematically observed for the $Asp^{70} \rightarrow$ Ala precursor and α-polypeptides. This increased mobility of the mutated polypeptides probably results from increased SDS-binding. The folding of these mutants should be nearly normal, since the K_m values are close to that of the WT and no dramatic accumulation of the precursor was observed (Table 1). The reason for the delayed activation of the precursor may be that the folding rate of the mutant polypeptides is slightly lower, which results in problems during autocatalysis. Combined quantum chemical calculations and molecular dynamics simulations have suggested that Asp^{70}, Lys^{230} and Arg^{234} are key transition-state-stabilizing residues in AGA-catalysed hydrolysis of the amide bond of a substrate [40]. Asp^{70} and Lys^{230} have no direct contact with the transition state atoms, but being charged residues, they could have a stabilizing electrostatic interaction. A similar role in autocatalysis can be proposed for these two residues.

Asn^{225} is a neighbouring residue of Thr^{206} stabilizers, Ser^{72} and Thr^{224}. We show here that the $Asn^{225} \rightarrow$ Ala mutation delays the processing of the precursor polypeptide (Figures 3 and 4). Although the K_m value was higher than for WT AGA, the V_{max} value remained normal (Table 1). In the case of $Asn^{225} \rightarrow$ Ala and $Lys^{230} \rightarrow$ Ala, decreased affinity for the substrate would indicate slight changes in the substrate-binding residues of the active site, whereas the catalytic machinery remained normal as indicated by the WT-level V_{max} value. The side-chain nitrogen of Asn^{225} (Ser^{171}) creates a hydrogen bond to the carbonyl oxygens of Gly^{71} (Arg^{49}) and Gly^{74} (Gly^{52}). In bacterial AGA, only the Ser^{171}–Arg^{49} hydrogen bond exists. The role of Asn^{225} is probably structural – it keeps the local structure stable and precise. Apparently, precursor accumulation and decrease of substrate binding capacity of the $Asn^{225} \rightarrow$ Ala mutant is the result of a local structural change.

The consequences at the polypeptide level were similar concerning the novel $Asp^{200} \rightarrow$ Ala and $Asp^{201} \rightarrow$ Ala substitutions (Figure 3). There was only a slight decrease in autocatalysis and polypeptides had normal kinetic values as well as normal intracellular targeting (Table 1). In immunofluorescence, the intracellular localization of all these novel mutants remained seemingly normal. Changes in K_m values would imply minor differences in substrate-binding capacity and thus perhaps in the structure of the active site of the mutant polypeptides (Table 1). Among the mutations studied in the present study, only $Thr^{33} \rightarrow$ Ala had no effect on AGA activation, whereas the kinetic values were affected, indicating a possible structural role for this residue in substrate hydrolysis.

Previous data exist for additional mutations, some resulting in human AGU. The residues are part of the autocatalytic machinery and are shown in orange in Figure 2. Ser^{72} is hydrogen-bonded to the free amino group of Thr^{206} in the native AGA structure [24]. $Ser^{72} \rightarrow$ Ala mutation decreases the V_{max} value, but the K_m value and autoproteolysis are unaffected, implying that the active site gets correctly folded. Thus the hydrogen bond to Thr^{206} is required for efficient enzymic catalysis. In contrast, the $Ser^{72} \rightarrow$ Pro mutant precursor polypeptides, found in AGU patients, are not activated intracellularly [35]. The reason for accumulation of the precursor may be that the loop structure, which contains Ser^{72}, is unable to accommodate the rigid proline residue without disturbing packing [32]. Ser^{72} is hydrogen-bonded to the side chain of Thr^{224} (Thr^{170}) and the main-chain nitrogen of the next amino acid in the bacterial $Thr^{206} \rightarrow$ Ala ($Thr^{152} \rightarrow$ Ala) structure (PDB code 9gaa), thus stabilizing local structure at the active site.

$His^{204} \rightarrow Gly$ and $His^{204} \rightarrow Ser$ mutant polypeptides get only partially activated due to defective autocatalytic machinery. Compared with the WT enzyme, 30 % of activity exists, which is accounted for by the normally processed portion of AGA polypeptides [10,28,35]. His^{204} has an important role in the autoproteolysis. The imidazole ring of His^{204} could be packed against the ring of Trp^{34} and perhaps Phe^{36}, thus maintaining the proper geometry for the scissile peptide bond between Asp^{205} and Thr^{206} (Figure 1). Consequently, the role of Trp^{34} would also be structural, since the mutant polypeptides of Trp^{34} are not activated [25].

The mutants of Arg^{234}, a residue that binds the aspartate moiety of the substrate to the active AGA molecule, do not get activated. The role of Arg^{234} (Arg^{180}) in activation is structural, since it either stabilizes the autocatalytic reaction participants like that described for the bacterial precursor AGA structures [18] or it may have other interactions with the activation machinery.

Some accumulation of the precursor has been observed for the alanine mutant of the substrate binding Asp^{237} [24]. A slow folding process due to a structural role of Asp^{237} may account for the accumulation of the precursor polypeptide in the ER.

In enzyme catalysis, Thr^{257} forms the oxyanion hole with Gly^{258} [1]. $Thr^{257} \rightarrow Ala$ and the AGU-causing $Thr^{257} \rightarrow Ile$ mutant both result in abnormal processing of the precursor polypeptide equally as $Gly^{226} \rightarrow Asp$ [24,32]. In some bacterial precursor AGA structures (PDB codes 9gac and 9gaa), Thr^{257} (Thr^{203}) is hydrogen-bonded to the side chain of Asp^{205} (Asp^{151}), while in others (PDB codes 9gaf, 1p4k and 1p4v) the side-chain orientation of Asp^{205} is different. Furthermore, the conformation of the spacer peptide between the α- and β-subunits varies significantly between different precursor structures, although the structures are very similar in other parts of the molecules. The C^{α}-position (approx. 1 Å, where 1Å = 0.1 nm) and rotamer conformation of Thr^{257} also vary. Thus it would be quite speculative to conclude that the role of human AGA Thr^{257} is to properly orient the side-chain Asp^{205} with a hydrogen bond.

Current view of the autocatalytic mechanism of human AGA

The autocatalytic activation of Ntn-hydrolases represents an interesting phenomenon. The residues that are important for activation have been identified from precursor structures of proteasome [20], AGA [18], penicillin G acylase [14], cephalosporin acylase [12,21] and glutaryl 7-aminocephalosporanic acid acylase [19], although the actual ones are not clearly defined for proteasome and penicillin G acylase. The activation of AGA precursor and enzymic catalysis seem to be accomplished by the same amino acids, which makes the interpretation of experimental data complicated. However, information of the bacterial precursor crystal structures can be used to draw some conclusions. The overall sequence identity between human and bacterial AGA is 35 %, and even higher concerning active site residues. Thus their structures are similar, and especially their catalytic and autocatalytic activation mechanisms can be assumed to be very similar. Determined from the WT human (PDB code 1apy) and bacterial (PDB code 2gaw) structures, the rmsd for the backbone of 509 residues is 1.12 Å. Furthermore, the secondary and tertiary structures of the bacterial mature AGA (PDB code 2gaw) [41] and precursor AGA (PDB code 9gaf) [18] are essentially identical (rmsd = 0.58 Å for the backbone of 547 residues). Thus it is conceivable that the precursor structures of the human and bacterial AGA are closely related. Consequently, the activation mechanisms are likely to be similar.

Five bacterial AGA precursor structures have been solved by crystallography (PDB codes 9gaa, 9gac, 9gaf, 1p4k and 1p4v). The structures are very similar, except at the linker peptide between the subunits and some neighbouring residues. The nucleophile location and rotamer conformation vary only slightly, but the position and conformation of the preceding residues, including Asp^{205}, are quite dissimilar. The new Asp^{205} (Asp^{151}) mutant structures (PDB codes 1p4k and 1p4v [42]), make it even more evident that, from only a few structures, it is speculative to make detailed conclusions about the residues that participate at each activation step. Thus more Ntn-hydrolase precursor structures are needed to generate a model for the general activation mechanism.

The bacterial AGA activation mechanism [18] is concluded from the data obtained from three different structures (PDB codes 9gaa, 9gac and 9gaf). The structure of the linker peptide between the subunits of AGA varies quite significantly between different bacterial precursor mutant constructs, some of which have only recently been obtained. This complicates the interpretation of the data concerning individual residues. Therefore conclusion of the exact role of individual residues at each activation step would be somewhat speculative. From our experimental data, we conclude that the activation mechanism we proposed for human AGA [10] remains a valid reaction mechanism for human AGA autoproteolysis. The mechanism resembles the N → O acyl shift reported for the splicing of inteins [9]. In the present paper, the presented mechanism (Scheme 1) is based on the mutation data from a number of active-site residues of human AGA. In the mechanism, the nucleophile forms a covalent bond with the carbonyl carbon of the preceding residue, Asp^{205}. The nucleophile is activated by a general base, which is either the side chain of Asp^{205} or a water molecule, as discussed below. Most of the residues analysed in the present study do not have a distinct role in the autoproteolytic activation reaction, although they are important for the reaction. They surround the active site and form the necessary hydrogen-bond network to position and interact correctly with the residues that participate in the reaction. Our $Gly^{258} \rightarrow Ala$ mutant revealed the crucial structural role of Gly^{258} for activation. Several other structural residues were identified which had a milder effect on activation by altering the local structure in such a way that the residues participating in activation were displaced or existed in an inactive conformation.

With Thr^{1} as the nucleophile in proteasomal enzyme catalysis, a proton acceptor in the active site is required for activation of the hydroxyl group. A catalytic water molecule, seen in the high-resolution structures of all three active subunits of the yeast proteasome [43], is ideally positioned to act as the general base and promote the abstraction of the proton from the Thr^{1} hydroxyl group. In addition, a bound water molecule seems to initiate the autoproteolytic activation of cephalosporin acylase [21]. In AGA, the water molecule bound to Asp^{237} and Thr^{206} possibly also performs this role. In this case, Asp^{205} would have a role in the formation of main-chain distortion, which may trigger the cleavage of the scissile peptide bond. The conformational strain at the scissile peptide bond possibly results from oligomerization of precursor molecules in the ER. The strain is lessened by the substitution of structurally important residues. These mutants thus have defective autocatalytic machineries that delay the cleavage of the precursor (Figure 4). Figure 6 summarizes the roles of the analysed human AGA residues. Compared with the enzymic catalysis, the autocatalytic cleavage of the peptide bond seems to be less efficient [10,30]. It is worth emphasizing that, in eukaryotic cells, the activation of AGA occurs in the ER, whereas the enzymic catalysis takes place in the lysosomes, which could contribute to the lower efficiency of the autocatalytic cleavage when compared with the enzymic catalysis.

Although the human AGA shares sequence similarity with other Ntn-hydrolases only in certain secondary elements, the autoproteolytic activation process shares several features with

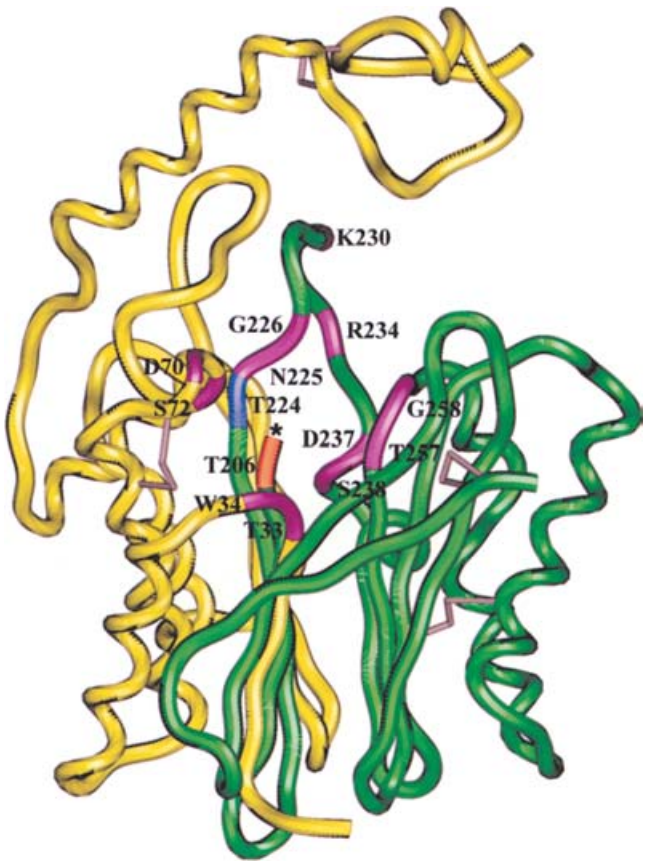

Figure 6 Residues that affect activation

The autocatalytic nucleophile is shown in orange. The residues which participate in autocatalysis are shown in blue, and the structural amino acids are shown in purple.

them [18–21]: (i) the overall structure of the precursor and the active molecule is very similar; (ii) the hydroxyl or sulphydryl group of the nucleophile, which functions both as the catalytic and autocatalytic nucleophile, is oriented towards the scissile peptide bond; (iii) conformational strain exists in the precursor at the cleavage site; and (iv) water molecules are utilized in the activation process.

We thank Paula Hakala for excellent technical assistance. The study was supported by grants from The Sigrid Juselius Foundation, Center of Excellence in Disease Genetics of The Academy of Finland Grant 44870, The Rinnekoti Research Foundation, Espoo, Finland, and The Finnish Cultural Foundation.

REFERENCES

1 Oinonen, C., Tikkanen, R., Rouvinen, J. and Peltonen, L. (1995) Three-dimensional structure of human lysosomal aspartylglucosaminidase. Nat. Struct. Biol. **2**, 1102–1108
2 Löwe, J., Stock, D., Jap, B., Zwickl, P., Baumeister, W. and Huber, R. (1995) Crystal structure of the 20 S proteasome from the archaeon *T. acidophilum* at 3.4 Å resolution. Science **268**, 533–539
3 Smith, J. L., Zaluzec, E. J., Wery, J. P., Niu, L., Switzer, R. L., Zalkin, H. and Satow, Y. (1994) Structure of the allosteric regulatory enzyme of purine biosynthesis. Science **264**, 1427–1433
4 Duggleby, H. J., Tolley, S. P., Hill, C. P., Dodson, E. J., Dodson, G. and Moody, P. C. E. (1995) Penicillin acylase has a single-amino-acid catalytic centre. Nature (London) **373**, 264–268
5 Suresh, C. G., Pundle, A. V., SivaRaman, H., Rao, K. N., Brannigan, J. A., McVey, C. E., Verma, C. S., Dauter, Z., Dodson, E. J. and Dodson, G. G. (1999) Penicillin V acylase crystal structure reveals new Ntn-hydrolase family members. Nat. Struct. Biol. **6**, 414–416
6 Kim, Y., Yoon, K., Khang, Y., Turley, S. and Hol, W. G. (2000) The 2.0 Å crystal structure of cephalosporin acylase. Struct. Fold. Des. **8**, 1059–1068
7 Lee, Y. S., Kim, H. W. and Park, S. S. (2000) The role of α-amino group of the N-terminal serine of β subunit for enzyme catalysis and autoproteolytic activation of glutaryl 7-aminocephalosporanic acid acylase. J. Biol. Chem. **275**, 39200–39206
8 Perler, F. B., Davis, E. O., Dean, G. E., Gimble, F. S., Jack, W. E., Neff, N., Noren, C. J., Thorner, J. and Belfort, M. (1994) Protein splicing elements: inteins and exteins – a definition of terms and recommended nomenclature. Nucleic Acids Res. **22**, 1125–1127
9 Shao, Y., Xu, M. Q. and Paulus, H. (1996) Protein splicing: evidence for an N-O acyl rearrangement as the initial step in the splicing process. Biochemistry **35**, 3810–3815
10 Saarela, J., Laine, M., Tikkanen, R., Oinonen, C., Jalanko, A., Rouvinen, J. and Peltonen, L. (1998) Activation and oligomerization of aspartylglucosaminidase. J. Biol. Chem. **273**, 25320–25328
11 Lee, Y. S. and Park, S. S. (1998) Two-step autocatalytic processing of the glutaryl 7-aminocephalosporanic acid acylase from *Pseudomonas* sp. strain GK16. J. Bacteriol. **180**, 4576–4582
12 Kim, Y., Kim, S., Earnest, T. N. and Hol, W. G. (2002) Precursor structure of cephalosporin acylase: insights into autoproteolytic activation in a new N-terminal hydrolase family. J. Biol. Chem. **277**, 2823–2829
13 Li, S., Smith, J. L. and Zalkin, H. (1999) Mutational analysis of *Bacillus subtilis* glutamine phosphoribosylpyrophosphate amidotransferase propeptide processing. J. Bacteriol. **181**, 1403–1408
14 Hewitt, L., Kasche, V., Lummer, K., Lewis, R. J., Murshudov, G. N., Verma, C. S., Dodson, G. G. and Wilson, K. S. (2000) Structure of a slow processing precursor penicillin acylase from *Escherichia coli* reveals the linker peptide blocking the active-site cleft. J. Mol. Biol. **302**, 887–898
15 Schmidtke, G., Kraft, R., Kostka, S., Henklein, P., Frömmel, C., Löwe, J., Huber, R., Kloetzel, P. M. and Schmidt, M. (1996) Analysis of mammalian 20 S proteasome biogenesis: the maturation of β-subunits is an ordered two-step mechanism involving autocatalysis. EMBO J. **15**, 6887–6898
16 Brannigan, J. A., Dodson, G., Duggleby, H. J., Moody, P. C., Smith, J. L., Tomchick, D. R. and Murzin, A. G. (1995) A protein catalytic framework with an N-terminal nucleophile is capable of self-activation. Nature (London) **378**, 416–419
17 Oinonen, C. and Rouvinen, J. (2000) Structural comparison of Ntn-hydrolases. Protein Sci. **9**, 2329–2337
18 Xu, Q., Buckley, D., Guan, C. and Guo, H. C. (1999) Structural insights into the mechanism of intramolecular proteolysis. Cell **98**, 651–661
19 Kim, J. K., Yang, I. S., Rhee, S., Dauter, Z., Lee, Y. S., Park, S. S. and Kim, K. H. (2003) Crystal structures of glutaryl 7-aminocephalosporanic acid acylase: insight into autoproteolytic activation. Biochemistry **42**, 4084–4093
20 Ditzel, L., Huber, R., Mann, K., Heinemeyer, W., Wolf, D. H. and Groll, M. (1998) Conformational constraints for protein self-cleavage in the proteasome. J. Mol. Biol. **279**, 1187–1191
21 Yoon, J., Oh, B., Kim, K., Park, J., Han, D., Kim, K. K., Cha, S. S., Lee, D. and Kim, Y. (2004) A bound water molecule is crucial in initiating auto-catalytic precursor activation in a N-terminal hydrolase. J. Biol. Chem. **279**, 341–347
22 Kasche, V., Lummer, K., Nurk, A., Piotraschke, E., Rieks, A., Stoeva, S. and Voelter, W. (1999) Intramolecular autoproteolysis initiates the maturation of penicillin amidase from *Escherichia coli*. Biochim. Biophys. Acta **1433**, 76–86
23 Choi, K. S., Kim, J. A. and Kang, H. S. (1992) Effects of site-directed mutations on processing and activities of penicillin G acylase from *Escherichia coli* ATCC 11105. J. Bacteriol. **174**, 6270–6276
24 Tikkanen, R., Riikonen, A., Oinonen, C., Rouvinen, R. and Peltonen, L. (1996) Functional analyses of active site residues of human lysosomal aspartylglucosaminidase: implications for catalytic mechanism and autocatalytic activation. EMBO J. **15**, 2954–2960
25 Riikonen, A., Tikkanen, R., Jalanko, A. and Peltonen, L. (1995) Immediate interaction between the nascent subunits and two conserved amino acids Trp^{34} and Thr^{206} are needed for the catalytic activity of aspartylglucosaminidase. J. Biol. Chem. **270**, 4903–4907
26 Wang, Y. and Guo, H. C. (2003) Two-step dimerization for autoproteolysis to activate glycosylasparaginase. J. Biol. Chem. **278**, 3210–3219
27 Riikonen, A., Rouvinen, J., Tikkanen, R., Julkunen, I., Peltonen, L. and Jalanko, A. (1996) Primary folding of aspartylglucosaminidase: significance of disulfide bridges and evidence of early multimerization. J. Biol. Chem. **271**, 21340–21344
28 Ikonen, E., Julkunen, I., Tollersrud, O. K., Kalkkinen, N. and Peltonen, L. (1993) Lysosomal aspartylglucosaminidase is processed to the active subunit complex in the endoplasmic reticulum. EMBO J. **12**, 295–302
29 Aula, P., Jalanko, A. and Peltonen, L. (2001) Aspartylglucosaminuria. In The Metabolic and Molecular Bases of Inherited Disease, (Scriver, C. R., Beaudet, A. L., Sly, W. S., Valle, D., Childs, B., Vogelstein, B. and Kinzler, K. W., eds.), pp. 3535–3550, McGraw-Hill, New York
30 Guan, C., Liu, Y., Shao, Y., Cui, T., Liao, W., Ewel, A., Whitaker, R. and Paulus, H. (1998) Characterization and functional analysis of the *cis*-autoproteolysis active center of glycosylasparaginase. J. Biol. Chem. **273**, 9695–9702

31 Stacey, A. and Schnieke, A. (1990) SVpoly: a versatile mammalian expression vector. Nucleic Acids Res. **18**, 2829
32 Saarela, J., Laine, M., Oinonen, C., von Schantz, C., Jalanko, A., Rouvinen, J. and Peltonen, L. (2001) Molecular pathogenesis of a disease: structural consequences of aspartylglucosaminuria mutations. Hum. Mol. Genet. **10**, 983–995
33 Halila, R., Baumann, M., Ikonen, E., Enomaa, N. and Peltonen, L. (1991) Human leucocyte aspartylglucosaminidase: evidence for two different subunits in a more complex native structure. Biochem. J. **276**, 251–256
34 Laemmli, U. K. (1970) Cleavage of structural proteins during the assembly of the head of bacteriophage T4. Nature (London) **227**, 680–685
35 Peltola, M., Tikkanen, R., Peltonen, L. and Jalanko, A. (1996) Ser72Pro active-site disease mutation in human lysosomal aspartylglucosaminidase: abnormal intracellular processing and evidence for extracellular activation. Hum. Mol. Genet. **5**, 737–743
36 Reissig, J. L., Strominger, J. L. and Leloir, K. M. (1955) A modified colorimetric method for the estimation of N-acetylamino sugars. J. Biol. Chem. **217**, 959–966
37 Spaete, R. R. and Mocarski, E. S. (1985) Regulation of cytomegalovirus gene expression: α and β promoters are trans activated by viral functions in permissive human fibroblasts. J. Virol. **56**, 135–143
38 Brogdon, W. G. and Dickinson, C. M. (1983) A microassay system for measuring esterase activity and protein concentration in small samples and in high-pressure liquid chromatography eluate fractions. Anal. Biochem. **131**, 499–503
39 Liu, Y., Guan, C. and Aronson, Jr, N. N. (1998) Site-directed mutagenesis of essential residues involved in the mechanism of bacterial glycosylasparaginase. J. Biol. Chem. **273**, 9688–9694
40 Peräkylä, M. and Kollman, P. A. (1997) A simulation of the catalytic mechanism of aspartylglucosaminidase using *ab initio* quantum mechanics and molecular dynamics. J. Am. Chem. Soc. **119**, 1189–1196
41 Guo, H. C., Xu, Q., Buckley, D. and Guan, C. (1998) Crystal structures of *Flavobacterium* glycosylasparaginase: an N-terminal nucleophile hydrolase activated by intramolecular proteolysis. J. Biol. Chem. **273**, 20205–20212
42 Qian, X., Guan, C. and Guo, H. C. (2003) A dual role for an aspartic acid in glycosylasparaginase autoproteolysis. Structure **11**, 997–1003
43 Groll, M., Ditzel, L., Löwe, J., Stock, D., Bochtler, M., Bartunik, H. D. and Huber, R. (1997) Structure of 20 S proteasome from yeast at 2.4 Å resolution. Nature (London) **386**, 463–471

Received 30 September 2003/13 November 2003; accepted 17 November 2003
Published as BJ Immediate Publication 17 November 2003, DOI 10.1042/BJ20031496